



Title	Improvement of Toughness of Weld Metal by High Heat Input Electroslag Welding Process (Part 3) (Materials, Metallurgy & Weldability)
Author(s)	Matsuda, Fukuhisa; Kikuchi, Yasushi; Fujihira, Shoichiro et al.
Citation	Transactions of JWRI. 1993, 22(2), p. 281-288
Version Type	VoR
URL	<a href="https://doi.org/10.18910/7584">https://doi.org/10.18910/7584</a>
rights	
Note	

*The University of Osaka Institutional Knowledge Archive : OUKA*

<https://ir.library.osaka-u.ac.jp/>

The University of Osaka

# Improvement of Toughness of Weld Metal by High Heat Input Electroslag Welding Process(Part 3) †

Fukuhisha MATSUDA\*, Yasushi KIKUCHI\*\*,  
Shoichiro FUJIHARA\*\*\*, and Zhong-dong QIAN\*\*\*\*

## Abstract

*The purpose of this report is to conduct various investigations and examinations for the improvement of impact characteristics of ES weld metal using different types of welding wire.*

*In this experiment, six types of welding wire are used by changing welding heat input to three levels such as  $Q = 456, 790$  and  $1,207$  KJ/cm.*

*The summary of the test results obtained are as in the following.*

- (1) *In the case of all three heat input levels, the impact test value in center location (C) of ES weld metal is generally lower than those in periphery locations (R). Furthermore, regardless of the types of welding wires, the same tendency has been noticed.*
- (2) *The possibility to improve the EA value in C location of weld metal which has been produced in the standard heat input such as  $Q = 456$  KJ/cm using Ni containing wire is found.*

**KEY WORDS :** (Weld Metal Toughness) (Electron-Slag Welding) (Low Carbon Steel)

## 1. Preface

Nowadays, lots of four-side thick plate box columns apply to the steel structures for general multistoried buildings, etc. In the automatic box column manufacturing line which intends the automatization of welding work and less dependence on worker's performance ability, significantly higher heat input welding process than those by conventional welding processes heavy current submerged arc welding process (hereafter called SAW) and electroslag welding process (hereafter called ESW) are used.

The purpose of this report is to clarify the impact characteristics, etc. of the weld metal produced by these high heat input ESW and to increase and improve the toughness of the weld metal. Mainly, the thick high tensile steel plates of 50 kg grade (SM490A, 40mm or over) are used for the test.

In this report, the improvement conditions for impact characteristics of both C (center of weld metal called Core zone) and R (periphery of weld metal called Rim zone) parts in the weld metal produced by various welding wires has been studied and investigated. The amount of welding heat input [hereafter called  $Q$  (KJ/cm)] is changed in three levels ( $Q = 456 \sim 1,267$  KJ/cm) and 6 types of welding wires including conventional ones are used for comparison. Moreover, for the sake of the improvement of the difference of absorption energy values (hereafter called EA value) of weld metal between C and R parts as well as the

comparison of impact characteristics of the weld metals produced by various welding wires, the micro-structure of various weld metals has fractographically been examined and studied.

## 2. Experiment method

### 2.1 Test piece

The chemical compositions of both steel test piece and ESW wires which are used for this test are shown in Table 1. The steel test piece is SM490A plates of 40mm thickness and six types of ESW wires including the ones on the market are compared. For A-F wires, the flux of molten type (brand name: YF15) is used.

**Table 1** Chemical compositions of test piece and wires (wt %)

Composition		C	Si	Mn	P	S	Cu	Ni	Mo
Materials									
SM490A									
	(40mmt)	0.16	0.43	1.42	0.011	0.004	—	—	—
ESW-Wire (1.6mmφ)	A	0.06	0.42	1.20	0.000	0.002	0.22	—	0.20
	B	0.10	0.07	1.78	0.010	0.002	0.22	—	0.50
	C	0.08	0.16	2.04	0.007	0.002	0.22	0.80	0.44
	D	0.05	0.01	1.88	0.018	0.004	0.19	—	0.31
	E	0.03	0.50	1.64	0.004	0.008	—	1.24	0.35
	F	0.04	0.29	1.23	0.007	0.008	—	4.18	0.21

† Received on December 20, 1993

\* Professor

\*\* Associate Professor

\*\*\* Co-operative Researcher, Katayama Str-Techs. Ltd.

\*\*\*\* Graduate Student

Transactions of JWRI is published by Welding Research Institute, Osaka University, Ibaraki, Osaka 567, Japan

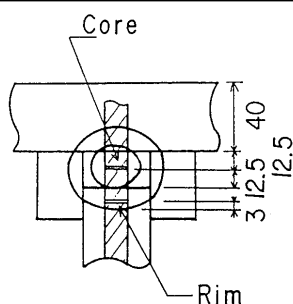
The element contents such as Si, Mn, Mo and Ni, etc. vary for six types of wires whose diameter is 1.6mm $\phi$ .

Wire B contains 0.5% Mo and wire D is of low silicon type (0.01% Si). Mainly, Ni content is changed for wires C, E and F (0.08%, 1.24% and 4.18% respectively.)

## 2.2 ESW welding parameters

Table 2 ESW welding parameters

E	T.P.			Welding speed	Diaph.	Gap	Q
S	Mark	I (A)	V (v)	(cm/min)	tD (mm)	G(mm)	(KJ/cm)
W	S	880	48	2.4	40	25	458
	M		50	1.5	60	25	790
	L		51	0.9	80	25	1,267



ESW welding parameters which are used for this test are shown in Table 2. The three levels of welding heat input such as  $Q = 456, 790$  and  $1,267$  KJ/cm are used. The amount of  $Q$  is changed by varying diaphragm thicknesses from 40 to 60mm and then to 80mm. Furthermore, the welding heat input of  $Q = 456$  J/cm is generally used as the standard ESW welding conditions.

The impact characteristics of C and R parts of the ESW weld metals produced with respective welding wires are checked.

## 2.3 Impact test method

Impact test is generally carried out at 0°C using the standard 2mm V notch Charpy test piece (10mm square). The notch positions in the ESW weld metal impact test pieces of C and R parts are shown in the figure below Table 2. The notch locations in the test piece of C and R parts are in the center of weld metal and within 3mm in weld metal from the bond.

## 2.4 Analysis of weld metal and microscopy of its structure

Main five elements such as C, Si, Mn, P and S as well as Mo and Ni in ESW weld metal of C and R parts are analyzed by mainly spectrochemical analysis. Furthermore, both oxygen ( $O_2$ ) and Nitrogen ( $N_2$ ) are analyzed by chemical analysis.

The fracture surface of impact test pieces is checked with SEM (scanning type electron microscope) and their microstructures are by optical microscopes after nital-etching.

Moreover, the welding heat cycle of C and R parts

(cooling characteristics) is measured using W-W-Re thermocouple. The weld metal temperature of C and R parts is measured by inserting the top of thermocouple into the molten metal at the end of weld seam immediately after finishing welding work.

## 3. Impact test results

### 3.1 Effect of welding heat input on weld metal impact characteristics of C and R parts

The examples of macro-structure photographs of both cross and longitudinal sections of the weld metals produced by commercial wire (A wire) and welding heat input of  $Q = 456$  and  $1,267$  KJ/cm are shown in Fig. 1. The difference of structure between C and R parts in the weld metal produced by  $Q = 456$  KJ/cm (40mm thickness, standard conditions) can be noticed. In other words, it can be seen that the prior austenite grains become finer at C part and coarser at R part of the weld metal produced by  $Q = 456$  KJ/cm, respectively.

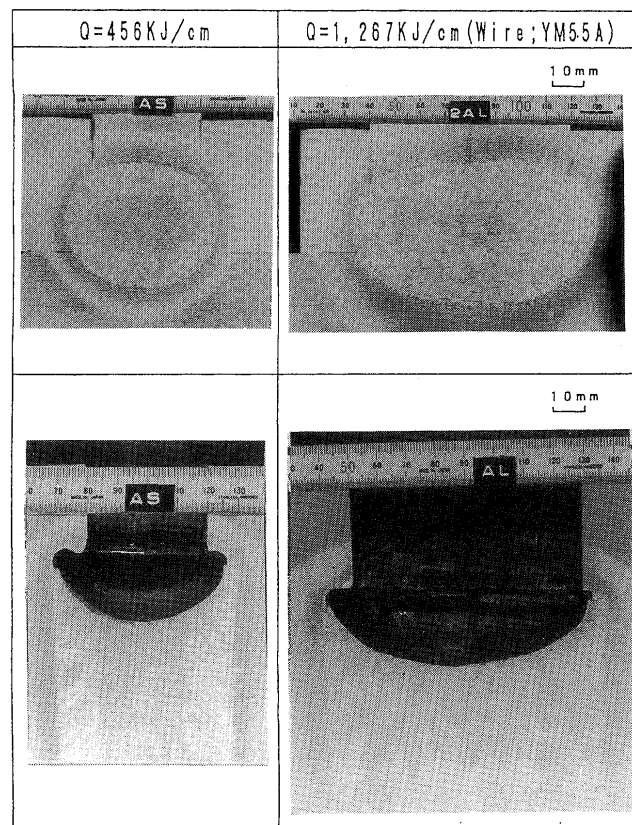


Fig. 1 Examples of weld metal macro-structure

On the other hand, it is noticed that there is not any difference of grain sizes between C and R parts of the weld metal produced by  $Q = 1,267$  KJ/cm but both of them become coarser. Furthermore, the tendency of grain growth at both C and R parts is found to be the same as that at both C and R parts of the weld metal produced by  $Q = 790$  KJ/cm. Only in the weld metal produced by  $Q = 456$  KJ/cm, the difference of grain size (prior austenite grain size) between C and R parts is noticed.

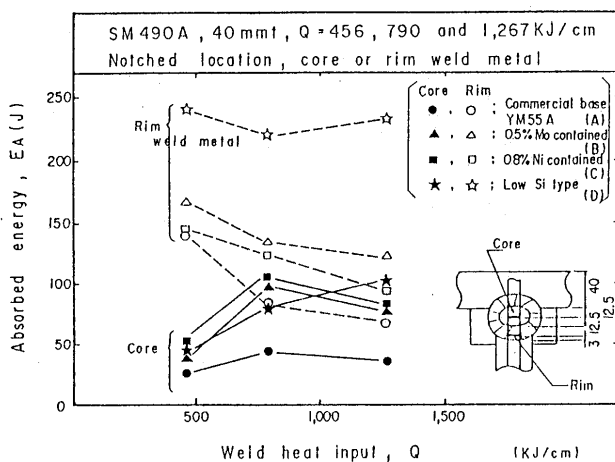


Fig. 2 Effect of  $Q$  on weld metal impact characteristics of both C and R parts

Fig. 2 shows the comparison of effects of  $Q$  on weld metal EA values by respective wires for C and R parts. For all welding heat input levels, the tendency is noticed that the EA values at C part are lower than those at R part. Especially, the difference is significant in the case of  $Q = 456$  KJ/cm.

For welding wires A, B and C and by  $Q = 790$  and  $1,267$  KJ/cm, the EA value of weld metal at C part is a little bit lower than that at R part but there is not any significant difference noticed between them.

Furthermore, there is no significant improvement noticed of EA value at C part of the weld metal by wires A~D and  $Q = 456$  KJ/cm.

The results of C part show that the EA values in the case of  $Q = 456$  KJ/cm are lower than those in other welding heat input levels for all wires. The EA value of the weld metal produced by D wire of low Si type is higher than others in the case of  $Q = 1,267$  KJ/cm.

The results of R part indicate the decreasing tendency of EA value according to the increase of  $Q$  for respective wires from A to D and the effect of  $Q$  on EA value is confirmed.

The EA value of weld metal by wire D of low Si type is significantly higher than other EA values. However, there is no difference noticed among the EA values by various welding wires.

### 3.2 Effect of additional welding wires (E, F) on weld metal impact characteristics at both C and R parts

Fig. 3 shows the comparison of EA values between C and R parts of the weld metals produced by the welding wires of six types including E, F wires used for this test and standard welding heat input of  $Q = 456$  KJ/cm.

A significant difference of EA values can clearly be noticed between C and R parts for all welding wires.

The possibility to improve the EA value of weld metal at C part is found from the results of C part of the weld metal produced by wires E and F (containing Ni of 1.24 wt% and 4.18 wt%, respectively).

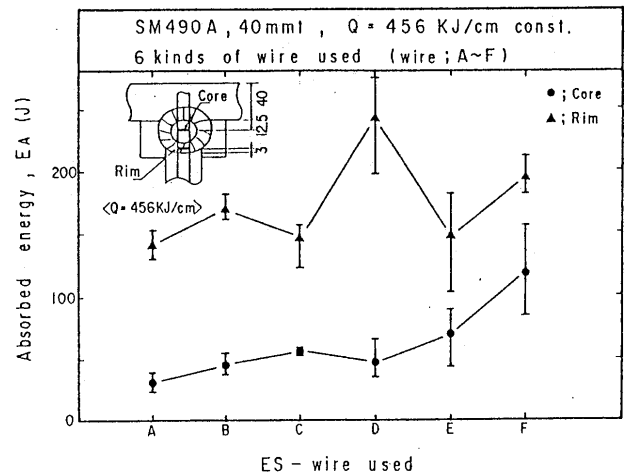


Fig. 3 Impact characteristics of weld metals by various welding wires

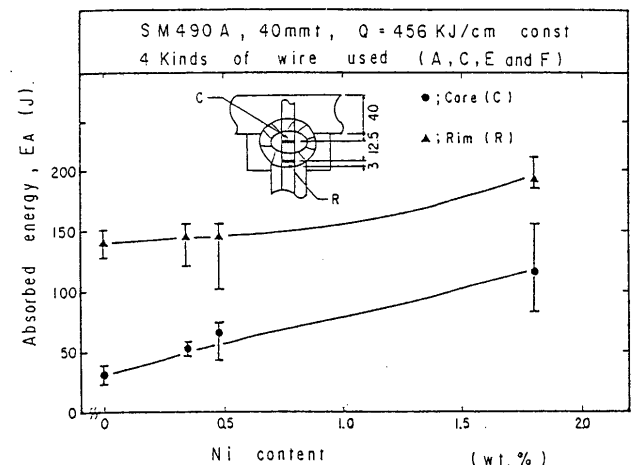


Fig. 4 Relation between EA value and Ni content of weld metal

Fig. 4 shows the relation between Ni contents of the weld metals produced by wires A, C, E and F and their EA values ( $Q = 456$  KJ/cm).

The relation between Ni content in weld metals and EA values is checked together with the analytical results of Ni content in the wires which is described later. The EA value at C part increases according to the increase of Ni content in weld metal and the same tendency is also noticed at R part.

Fig. 5 shows the comparison of examples of macrostructures in crosssection of the weld metals produced by both conventional commercial-base wire (wire A) and Ni containing wire (wire F containing Ni of 4.18 wt%). Because of the increase of Ni content, there is not any or so limited generation of fine grain zone found at C part but only coarse grain zone. It seems that the disappearance of fine grain zone from C part causes the improvement of EA value.

As stated above, for the improvement of impact characteristics at C part of the weld metal produced by standard heat input ( $Q = 456$  KJ/cm), it is confirmed that the addition of Ni is effective within the scope of experiment of this time.

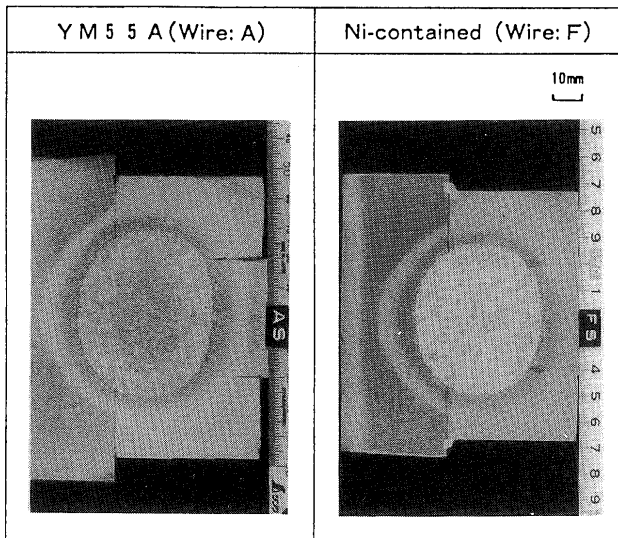


Fig. 5 Comparison of macrostructures in cross sections of weld metals produced by commercial-base wire and Ni containing wire ( $Q = 456$  KJ/cm)

#### 4. Discussion on the difference of EA values

##### 4.1 EA values at C and R parts

In this clause, the difference of EA values of the weld metals produced by standard welding heat input ( $Q = 456$  KJ/cm) between C and R parts will be discussed.

Table 3 shows the comparison of chemical and gas compositions between C and R parts of the weld metals produced by standard welding heat input of  $Q = 456$  KJ/cm and were A. As for main five elements and gas compositions, there is no significant difference of them found between C and R parts of ESW weld metal.

Table 3 Chemical composition of weld metal at C and R parts (wt%)

Location	C	Si	Mn	P	S	O*	N*
Core	0.11	0.40	1.46	0.012	0.004	112	46
Rim	0.11	0.39	1.44	0.011	0.004	109	47

\*PPM

Fig. 6 shows the room temperature structures (microstructures X100) at both C and R parts of the weld metal produced by standard welding heat input of  $Q = 456$  KJ/cm.

Judging from the type of grain boundary ferrite (GBF) at both C and R parts of weld metal and based on their microstructures, it is obvious that prior austenite ( $\gamma$ ) grains become finer or coarser.

Coarse GBF is generated in the fine grain boundaries of C part of weld metal (the former) and coarse polygonal ferrite (PF) of high density is generated inside the grains. On the other hand, the generation of GBF in the coarse grain boundaries of R part of weld metal (the latter) and the generation of acicular ferrite (AF) inside the grains are noticed.

The significant difference of structures between C and

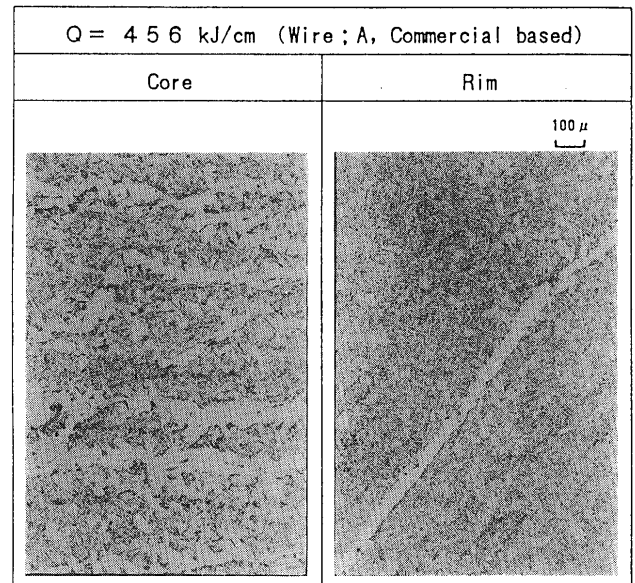


Fig. 6 Microstructures at C and R parts of weld metal by conventional welding wire (wire A)

R parts is caused by the generation quantity of coarse ferrite. It is noticed that both GBF and PF are generated in high density and only a little amount of AF exists in the case of C part. On the contrary, it is seen that only a little amount of GBF is generated in coarse prior-austenite ( $\gamma$ ) boundaries and lots of AF with a little amount of PF are generated inside the grains in the case of R part.

It seems that the difference of ferrite structure types causes a significant difference of EA values between C and R parts even in the same weld metal.

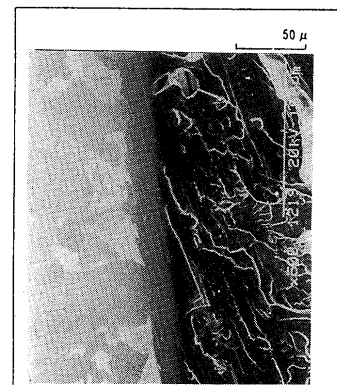


Fig. 7 SEM examination surface and fracture at C part of weld metal ( $Q = 1,267$  KJ/cm)

Fig. 7 shows both SEM examination surface and fracture at C part in the weld metal produced by ( $Q = 1,267$  KJ/cm). It is confirmed that the cracks in the impact fracture selectively propagate along coarse GBF.

This phenomenon is also confirmed by the observation of microstructure near the fracture with a microscope. Fig. 8 shows one of the examples where the primary cracks are generated along GBF at C part. The generation of secondary cracks along another GBF or PF can be seen. However, at R part the primary cracks are partly generated

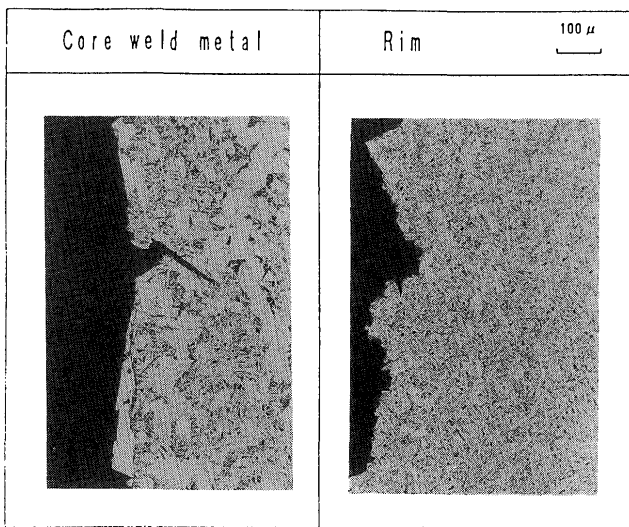


Fig. 8 Microstructure of fracture (C and R parts of weld metal)

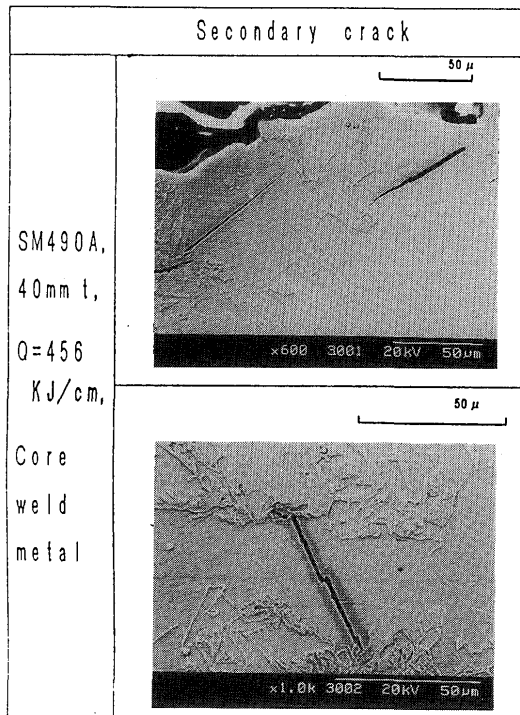


Fig. 9 Example of secondary cracks found with SEM

along GBF and there is not any secondary cracks found.

Furthermore, the enlargement of neighboring area of fracture with SEM in high magnification (X600 times or 1,000 times) also shows the generation of brittle secondary-cracks with no ductility inside GBF. One of them is shown in Fig. 9.

As the results of the above description, it seems that EA value at C part where the coarse ferrite is continuously generated in the grain boundaries as well as the inside of grains is generally low by the selective propagation of cracks like this.

Fig. 10 shows the examples of impact fracture with SEM (X400 times) at C and R parts of the weld metal pro-

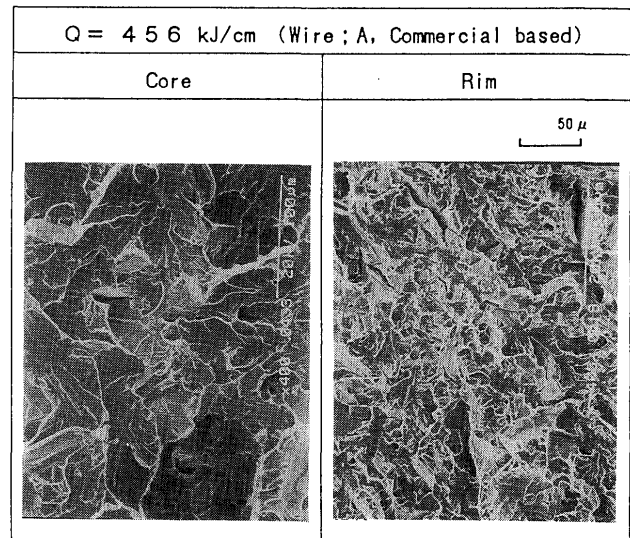


Fig. 10 Examples of impact fractures (comparison between C and R parts)

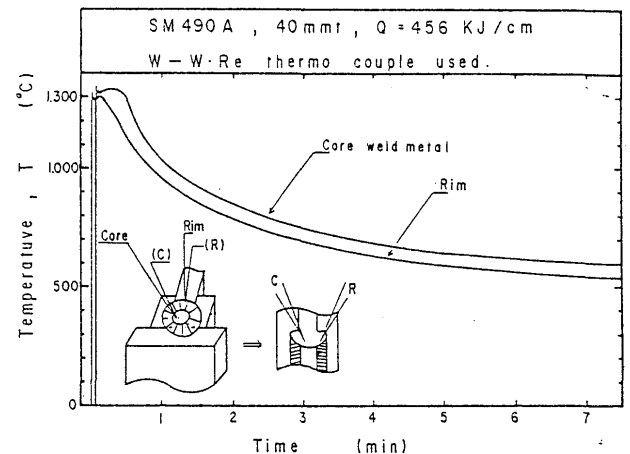


Fig. 11 Example of measured results of weld thermal cycle

duced by standard welding heat input of  $Q = 456$  KJ/cm.

The location of observation is about the center of respective impact test piece fractures (face of  $8 \times 10$  mm square). The EA values of impact fractures at both C and R parts are 25 and 130 J, respectively (at  $0^\circ\text{C}$ ).

It is confirmed that the facet size at C part is clearly larger than that at R part ( $50 - 100 \mu$  at C part and  $50 \mu$  or less at R part).

The cooling time of weld metal is measured in order to investigate the difference of microstructures between C and R parts. Fig. 11 shows the examples of measuring results of cooling characteristics at both C and R parts of the weld metal produced by the standard welding heat input of  $Q = 456$  KJ/cm using W-W-Re thermocouple. However, they are the measured results not of continuous welding but of molten metal just after the stop of ESW welding work.

Fig. 12 shows the comparison of cooling times ( $\tau_{t_1 \sim t_2}$ : sec) of the weld metals produced by the different welding heat input between  $Q = 456$  KJ/cm and  $Q = 1,267$  KJ/cm. No large difference of  $\tau_{1300 \sim 800^\circ\text{C}}$  is noticed be-

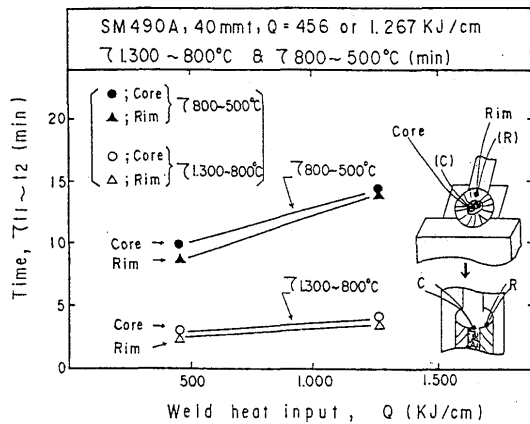


Fig. 12 Comparison of cooling time

tween C and R parts of weld metals produced by each welding heat input. On the other hand, the  $\tau_{800 \sim 500^\circ\text{C}}$  at C part of weld metal produced by  $Q = 456 \text{ KJ/cm}$  is a little bit larger than that at R part but the difference between these two cooling times is not so large to cause the change of microstructure of weld metal. The cooling times ( $\tau_{800 \sim 500^\circ\text{C}}$ ) at C and R parts are equivalent to a little less than 10 minutes and about 9 minutes, respectively.

Therefore, as a result it is considered that the microstructural difference between C and R of weld metal is not be caused by the difference of thermal cooling phenomena after welding.

#### 4.2 Change of EA values by different wires

Table 4 shows the chemical compositions of the weld metals produced by six types of welding wires and the standard welding heat input of  $Q = 456 \text{ KJ/cm}$ .

Table 4 Comparison of chemical compositions between wires and respective weld metals

								(wt%)	
Composition							Av. of		
Mark		C	Si	Mn	Mo	Ni	EA (J)	Remarks	
Base metal (SM490A, 40t)		0.15	0.43	1.42	—	—	—	—	
Wire	A	Wire	0.08	0.42	1.25	0.20	0.07	31	Commercial base
		EWS	0.11	0.42	1.49	0.08	0.03		
	B	Wire	0.10	0.07	1.78	0.60	0.07	45	0.5% Mo contained
		EWS	0.13	0.23	1.40	0.10	0.08		
	C	Wire	0.08	0.16	2.04	0.44	0.80	55	0.8% Ni contained
		EWS	0.12	0.31	1.62	0.18	0.34		
	D	Wire	0.05	0.01	1.66	0.31	0.06	49	Low Si type
		EWS	0.11	0.22	1.53	0.13	0.02		
	E	Wire	0.03	0.50	1.64	0.36	1.24	70	1.24% Ni contained
		EWS	0.10	0.44	1.47	0.13	0.48		
	F	Wire	0.04	0.29	1.23	0.21	4.19	115	4.18% Ni contained
		EWS	0.10	0.34	1.02	0.10	1.01		

The carbon content in weld metal (C: 0.10-0.13%) is a little higher than those in wires (C: 0.3-0.11%) owing to the dilution from base metal (C: 0.15 wt%).

On the other hand, Ni content in the weld metal produced by the wire containing 4.18% Ni (wire F) decreases to 1.81%. From this, the dilution from the base metal to weld metal is estimated to be 50% or more.

The contents of C, Mo and Ni in weld metals show the good relation with the dilution from the base metal. As for the contents of Si and Mn, the clear correlation among weld metals, base metals and wires can not be found owing to the slag reaction, etc.

Fig. 13 shows the comparison of respective microstructures at C part of weld metals produced by wire B containing 0.5% Mo and conventional wire (wire A).

The improvement of EA value can be expected by the addition of alloying elements such as Mo, etc. as the tendency to restrict and control the generation of coarse GBF is noticed.

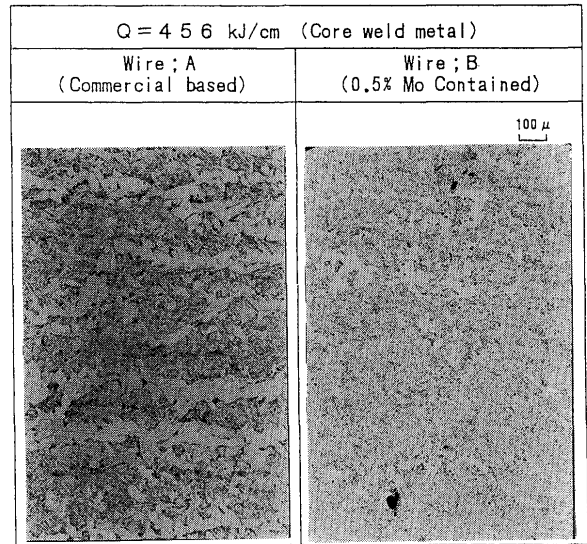


Fig. 13 Comparison of microstructures of weld metals produced by wire B containing 0.5% Mo and conventional wire (wire A)

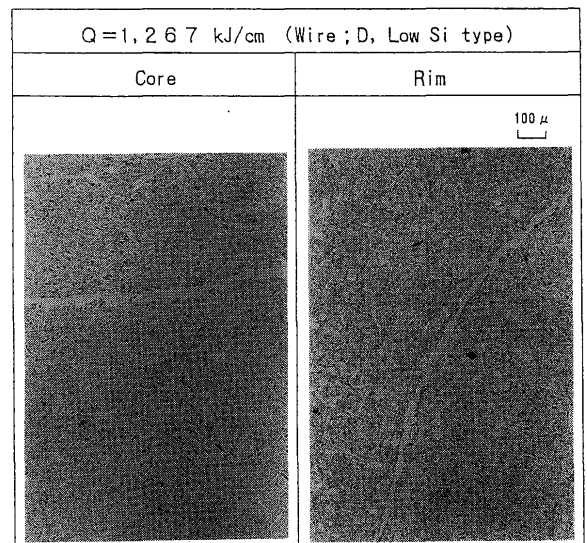


Fig. 14 Comparison of microstructures between C and R parts of weld metal produced by low Si type wire (wire D) and  $Q = 1,267 \text{ KJ/cm}$

Fig. 14 shows the comparison of microstructures between C and R parts of the weld metals produced by wire D containing low Si and welding heat input of  $Q = 1,267$  KJ/cm. The generation of coarse prior-austenite grains is found at both C and R parts. Furthermore, since the generation of a little PF together with a lot of fine AF inside the grains is noticed, high EA value can be expected.

The generation of coarse grains (prior  $\gamma$  grains) at both C and R parts is also noticed in the weld metal produced by welding heat input of  $Q = 790$  KJ/cm and this tendency is not related to the change of types of wires.

Fig. 15 shows the comparison of microstructures between C and R parts of the weld metal produced by the wire containing 4.18% Ni (wire F) and the welding heat input of  $Q = 456$  KJ/cm.

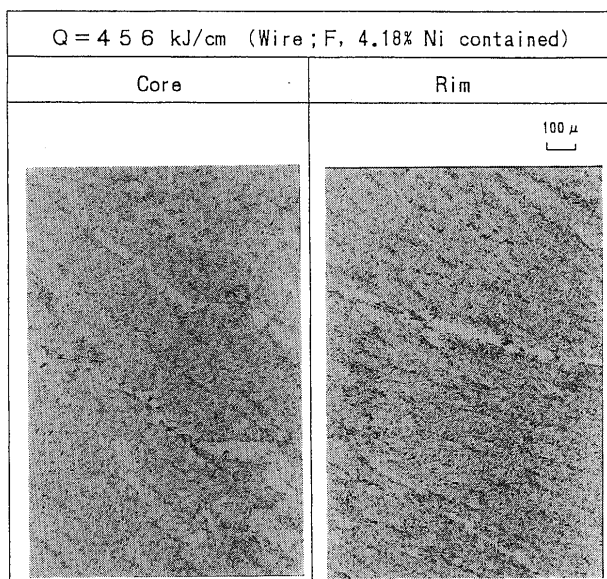


Fig. 15 Microstructures of weld metal produced by the wire containing 4.18% Ni and  $Q = 456$  KJ/cm.

The generation of coarse grains (prior  $\gamma$  grains) at both C and R parts is noticed by the addition of Ni element and there is no significant difference found between both microstructures. It can also be expected from Fig. 5 already shown that there is no significant difference of prior  $\gamma$  grain size between C and R parts.

Fig. 16 shows the comparison of impact fractures (with SEM) at C part of the weld metals produced by wire F containing Ni and conventional wire (wire A).

The facet size in the brittle fracture of weld metal produced by conventional wire is large but the dimple fracture is partly seen in the weld metal produced by the wire containing Ni so that the improvement of EA value can be expected.

For the study on the improvement of EA values, six types of wires are used in this experiments and it is found that the addition of Ni element (application of the wire containing Ni of a little more than 4%) is most effective for the improvement of EA values at C part of the weld metal produced by the standard welding heat input of  $Q = 456$  KJ/cm.

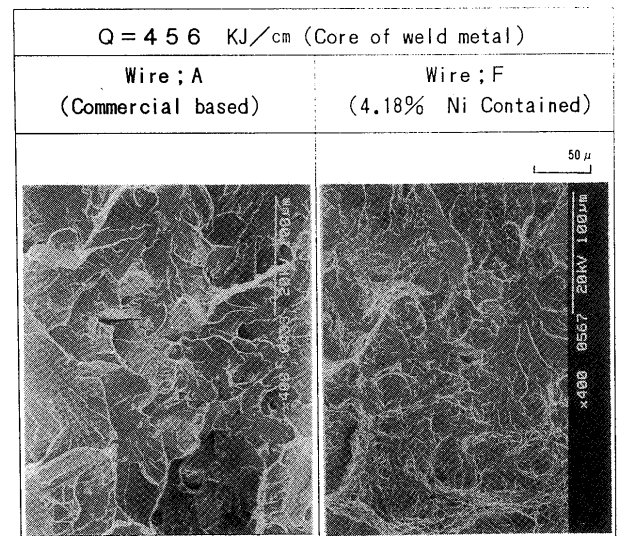


Fig. 16 Examples of impact fractures of the weld metal produced by the wire containing Ni.

## 6. Conclusions

For the purpose of improving the impact characteristics of ES weld metal produced by six types of welding wires, various studies and investigations have been carried out for this report.

Welding heat input has been changed to three levels such as  $Q = 456$ , 790 and 1,267 KJ/cm together with the change of six types of welding wires in the experiments of this time.

The results obtained will be summarized as in the following.

### [1] Summary of impact test results

- (1) The tendency to show that the EA values at C part of weld metals are generally lower than those at R part is noticed and this tendency has nothing to do with the types of wires which have been tested.
- (2) It is possible to improve EA value at C part of the weld metal produced by the wire containing Ni (wire F containing 4.18% Ni) and standard welding heat input of  $Q = 456$  KJ/cm.

### [2] Difference of EA values between C and R parts

- (1) By the results of studying microstructures, it is confirmed that the prior austenite ( $\gamma$ ) grains are fine at C part and coarse at R part, respectively.
- (2) The difference of EA values between C and R parts is significantly caused by the different of amount of ferrite between them. The generation of lots of polygonal (PF) in high density is noticed in C part (the former) and the generation of fine acicular ferrite (AF) in R part (the latter). These phenomena correspond with the difference of EA values between the former and the latter.

**[3] Relation between EA values and types of welding wires**

- (1) The analytical results of welding wires, base metal and weld metals show that the dilution from the base metal into weld metal is comparatively stable (about 50 ~ 60%) so far C, Mo and Ni contents are concerned.
- (2) It can be expected that the EA values at C part are improved by the addition of Ni element as the former austenite ( $\gamma$ ) grains become coarser. It has been confirmed that the addition of Ni element is more effective for the improvement and increase of EA values of ES weld metal. However, since the cost of this type of welding wire is high, the improvement of EA values by adding other elements are now under study.

**Acknowledgment**

Great cooperation given by Nittetsu Yousetsu Kogyo KK by tendering test pieces, etc. for the experiments of this time is deeply appreciated.

**References**

- 1) Hatanaka, Fujihira and Matsuda, "Research on Improvement of Toughness Characteristics of Weld Metal by High Heat Input Welding Process", Katayama Giho, No.11, P23-30 (1991).
- 2) S. Fujihira, A. Hatanaka, Y. Kikuchi and F. Matsuda, "An Investigation on Toughness Characteristics of Weld Metal of 50 Kg/mm<sup>2</sup> Class Constructional Steels by High Heat Input Electro-slag Welding Process", Pacrim Welcon, '92-DARWIN, Transferring Technology & Knowhow, Paper No.26, July, 1992.
- 3) Hatanaka, Fujihira, Matsuda and Kikuchi, "Fundamental Research on Improvement of Toughness Characteristics of Weld Metal by High Heat Input Welding Process-Electro-slag Welding (Part 2)", Katayama Giho, No.12, P28-35.
- 4) F. Matsuda, Y. Kikuchi, S. Fujihira and A. Hatanaka, "Microstructure and Toughness of High Heat input Electro-slag Weld Metal of 50 Kg/mm<sup>2</sup> Class Constructional steels", Transactions of JWRI (Osaka University), Vol.21, No.2, P93-99, 1992.